Cancer Letters 446 (2019) 1–14

Contents lists available at ScienceDirect

Cancer Letters

journal homepage: www.elsevier.com/locate/canlet

Original Articles

TIPE3 is a regulator of cell apoptosis in glioblastoma

Fanen Yuan[a,b], Baohui Liu[a,b], Yang Xu[a,b], Yuntao Li[a,c], Qian Sun[a,b], Pengfei Xu[a,b], Rongxin Geng[a,b], Gang Den[a,b], Jian Yang[a,b], Shenqi Zhang[a,b], Lun Gao[a,b], Jianming Liao[a,b], Junhui Liu[a,b], Xue Yang[a,b], Yinqiu Tan[a,b], Qianxue Chen[a,b,*]

[a] Department of Neurosurgery, Renmin Hospital of Wuhan University, Wuhan, Hubei, 430060, PR China
[b] Central Laboratory, Renmin Hospital of Wuhan University, Wuhan, Hubei, 430060, PR China
[c] Department of Neurosurgery, Huzhou Central Hospital, Huzhou, Zhejiang, 313000, PR China

ARTICLE INFO

Keywords:
TIPE3 p38 phosphorylation translocation apoptosis

ABSTRACT

Tumor necrosis factor alpha-induced protein 8-like 3 (TIPE3) is closely related to tumourigenesis and development. However, its role in human glioblastoma (GBM) and the underlying mechanisms remain unclear. In this study, we demonstrate that TIPE3 is upregulated in GBM, and its high expression predicts poor prognosis. TIPE3 depletion induces GBM cell apoptosis both in vitro and in vivo. Mechanism studies reveal that TIPE3 inhibits p38 phosphorylation and negatively regulates the p38 MAPK pathway. TIPE3 associates with p38. The nuclear translocation of p38 is blocked by TIPE3 overexpression. And p38 phosphorylation could regulate TIPE3-mediated p38 nuclear-cytopalsmic translocation but does not affect TIPE3-p38 association. Rescue experiments confirm that TIPE3 inhibits GBM cell apoptosis via the p38 MAPK pathway. In conclusion, TIPE3 inhibits p38 phosphorylation and blocks p38 nuclear translocation. This action thus negatively regulates the p38 MAPK pathway and results in GBM cell survival.

1. Introduction

Glioblastoma (GBM) is the most common and lethal primary brain tumour in adults. Although the standard therapeutic strategy, which includes surgery, chemotherapy and radiotherapy, is widely used, the median survival remains ~15 months [1,2]. This short survival time is attributed mainly to the highly mutated genome of GBM [3]. The comprehensive result of these genetic alterations is deregulated cell survival and death signalling pathways [4]. Therefore, there is an increasing need for investigating the mechanisms underlying the development and progression of GBM.

Tumor necrosis factor alpha-induced protein 8-like 3 (TIPE3, also known as TNFAIP8L3) is a newly identified member of the TNFAIP8 family [5]. Previous studies have shown that TIPE3 contains 7 highly conserved alpha helices (α0 ~ α6) and a hydrophobic cavity and is the transfer protein of phosphoinositide second messengers, which promote cancer [6]. Moreover, the TH domain of TIPE3 which contains 7 alpha helices is responsible for its lipid binding ability and subsequent AKT signalling activation, and the molecular alteration of TH domain affected its lipid binding activity and signalling transduction. TIPE3 is detectable in a wide range of human organs and is highly upregulated in several types of human cancer tissue, including oesophageal, lung, cervical, breast and colon tissue [6–9]. TIPE3 reportedly accelerates breast cancer metastasis by activating the AKT and NF-κB signalling pathways [8]. Fayngerts et al. found that TIPE3 promoted the growth and tumourigenesis of NIH3T3-HRasV12 cells through the PI3K-AKT and MEK-ERK pathways [6]. Interesting, it is reported that TIPE3 promotes the proliferation and migration of non-small cell lung cancer cells depending on its localization on plasma membrane, while cytoplasmic TIPE3 may exert a opposite effect [10]. Liu et al. found that TIPE3 hypermethylation correlates with worse prognosis and promotes tumor progression in nasopharyngeal carcinoma [11]. In a word, the function of TIPE3 is novel and rarely investigated. Moreover, the expression pattern and the role of TIPE3 in GBM remains unclear.

p38 MAPK is a crucial transducer of cellular stress signalling that consequently controls the balance between cell death and survival [12–14]. p38 signal activation is achieved via a cascade of phosphorylation events, including upstream MAP kinase kinase 3/6 (MKK3/6) [15]. Dual Thr180 and Tyr182 phosphorylation at the conserved TGY motif leads to p38 activation [16]. Hence, this phosphorylation is widely considered as a marker for p38 activation. Upon activation, phosphorylated p38 can activate many substrates, which include transcription factors, protein kinases, cytosolic and nuclear proteins [17], to exert subsequent downstream biological effects. As for the regulation of

* Corresponding author. Department of Neurosurgery, Renmin Hospital of Wuhan University, Wuhan, Hubei, 430060, PR China.
E-mail address: chenqx666@whu.edu.cn (Q. Chen).

https://doi.org/10.1016/j.canlet.2018.12.019
Received 19 August 2018; Received in revised form 29 November 2018; Accepted 27 December 2018

cell death, phosphorylated p38 activates transcription factors such as MEF2, ATF1 and CHOP, and the activation of these transcription factors lead to activation of cell death signals [17]. P38 MAPK is reported to be a proapoptotic inducer upon chemotherapy in many cancers [18], and its activation facilitate pro-apoptotic signalling cascades. Cyclophosphamide can induce apoptosis by activating p38 MAPK pathway in breast cancer [19]. The activation of p38 was reported to facilitate apoptotic pathway by inhibiting the expression of Bcl-2 in hepatoma [20]. It is reported that phosphorylated p38 can phosphorylate transcription factor MEF-2, resulting in mitochondrial depolarization and apoptosis [21]. When it comes to autophagy, p38 MAPK was reported to be a critical regulator of the balance between apoptosis and autophagy induced by 5-fluorouracil [22]. However, the role of p38 in cancer is complicated, and appears to be influenced by several factors, such as cell type, the extent of activation. In GBM, previous research has demonstrated that the p38 MAPK pathway plays a key role in the process of glioblastoma cell death induced by autophagy inhibitors and temozolomide [13]. Gao et al. found that the activation of p38 MAPK pathway mediates TNF-α-induced apoptosis in glioma [23]. The p38 MAPK pathway reportedly mediated Juglone-induced apoptosis in glioma stem-like cells [24]. P38 is usually considered as a pro-apoptotic inducer, but the inactivation of p38 MAPK was reported to inhibit to glioma cell invasion [25]. It reminds us that p38 MAPK may function in a cell type specific and context-dependent manner. Despite the critical role of p38 MAPK in GBM, its underlying mechanism remains to be fully elucidated.

In this study, we identify a novel role of TIPE3 as a regulator of apoptosis in GBM. We demonstrated that TIPE3 depletion induced GBM cell apoptosis both in vitro and in vivo. Mechanistically, TIPE3 inhibits p38 phosphorylation. TIPE3 associates with p38. The nuclear tranlocation of p38 is blocked by TIPE3 overexpression. The phosphorylation status of p38 is a critical regulator for TIPE3-mediated p38 nuclear-cytoplasmic translocation, but the phosphorylation of p38 is not required for the association between TIPE3 and p38. This effect negatively regulated the p38 MAPK signalling pathway and resulted in GBM cell survival.

2. Materials and methods

2.1. Bioinformatics

TIPE3 expression profiles in various human cancers was analyzed from TCGA database. Survival analysis (from the dataset “TCGA_GBM”) and Pearson correlation analysis (from the dataset “Bao”) were carried out by the GlioVis portal (http://gliovis.bioinfo.cnio.es) [26]. Gene set enrichment analysis (GSEA) was used to analyse the potential genes influenced by TIPE3, and this data (GSE4290) was downloaded from the Gene Expression Omnibus (GEO).

2.2. Human tissue samples

Human glioma and non-glioma tissues were collected from the Department of Neurosurgery, Renmin Hospital of Wuhan University, Wuhan, China. Non-glioma tissues were collected during surgery of severe traumatic brain injury after informed consent from the patients who needed post-trauma surgery. And the clinical glioma specimens were examined and diagnosed by pathologists at Renmin Hospital of Wuhan University. Tissue procurement and use in this study were performed with written patient informed consent and approved by the Institutional Ethics Committee of the Faculty of Medicine at Renmin Hospital of Wuhan University (approval number: 2012LKSZ (010) H).

2.3. RNA extraction and quantitative real-time PCR

Total RNA was extracted using Trizol reagent (Invitrogen, USA), and cDNA was synthesized using a PrimeScript RT Reagent Kit with gDNA Eraser (RR047A, Takara, Japan). Quantitative real-time PCR (qPCR) for TIPE3 mRNA levels was performed using SYBR® Premix Ex Taq™ II (RR820A, Takara) according to the manufacturer's instructions and an Applied Biosystems® 7500 Real-Time PCR System (Thermo Fisher Scientific, USA). GAPDH was used for normalization. The data were analyzed by the relative Ct method and expressed as a fold change compared with the control. The primer sequences included the following: TIPE3 5′- ACCCAAGCACACTGGTTTCC -3’ (Forward), 5‘- CTT GGGTCCCTGCATATCCG -3’ (Reverse); GAPDH 5′-GGAGCGAGATCCC TCCAAAAT-3’ (Forward), 5′-GGCTGTTGTCATACTTCTCATGG-3’ (Reverse).

2.4. Antibodies and reagents

The antibodies included the following: anti-TIPE3 (sc-249062, Santa Cruz Biotechnology, USA), anti-TIPE3 (#A14951, Boster Biological Technology, Wuhan, China), anti-p38 (#4511, Cell Signalling Technology, USA), anti-p-p38 (#9212, Cell Signalling Technology), anti-Bcl-2 (GTX100064, GeneTex, USA), anti-caspase-3 (GTX110543, GeneTex), anti-cleaved-caspase3(ab32042, Abcam, UK), anti-Bcl-xL (#2764, Cell Signalling Technology), anti-GAPDH (#5174, Cell Signalling Technology), anti-β-actin (#4970, Cell Signalling Technology), anti-α/β-tubulin (#2148, Cell Signalling Technology), anti-histone H3 (ab1791, Abcam), anti-HA (M180-3 and M561, Medical Biological Laboratories, Japan), anti-myc (M047-3 and M562, Medical Biological Laboratories) and anti-His (D291-3, Medical Biological Laboratories). The p38 MAPK inhibitor SB203580 was purchased from Selleck (S1076, USA), and the p38 MAPK inhibitor BIRB796 was obtained from TargetMol (T6277, USA).

2.5. Cell culture and treatment

Human glioblastoma cell lines (U251 and U87) and HEK 293T cells were obtained from the Cell Bank of the Shanghai Institute of Biochemistry and Cell Biology, Chinese Academy of Sciences (Shanghai, China). Cells were cultured in high-glucose DMEM (Gibco, Thermo Fisher Scientific) supplemented with 10% foetal bovine serum (Thermo Fisher Scientific) and 1% penicillin/streptomycin (Thermo Fisher Scientific). SB203580 was used at 20 μM. BIRB796 was used at 1 μM.

2.6. siRNA transfection

Specific siRNA targeting human TIPE3 (siTIPE3) and negative control siRNA (siNC) were obtained from RiboBio Corporation (Guangzhou, China). Transfection was done using X-tremeGENE siRNA transfection reagent (Roche, Germany) according to the manufacturer's protocol. The sequence of different siTIPE3 were showed below.

siTIPE3-1: 5′- CGCAGCAUGGAUUCGGAUU dTdT-3’ (sense) and 3’-dTdT GCGUCGUACCUAAGCCUAA-5’ (antisense).

siTIPE3-2: 5′- GGAACGUGCUCUCCAAUCU dTdT-3’ (sense) and 3’-dTdT CCUUGCACGAGAGGUUAGA -5’ (antisense).

2.7. DNA construction and transfection

Full-length TIPE3 cDNA was subcloned into the pcDNA3.1 vector with a HA tag (HA-TIPE3). N-terminal truncated TIPE3 cDNA was subcloned into the pIRES2-ZsGreen1 vector with a myc tag (myc-TIPE3). Full-length p38 cDNA was subcloned into the pcDNA3.1 vector with a 6xHis tag (His-p38). A dominant negative mutant (the TGY dual phosphorylation sites Thr180 and Tyr182 were both changed to AGF) of p38 was subcloned into the pcDNA3.1 vector with a 6 x His tag (His-mt-p38). Transfections were done using Lipofectamine 3000 transfection reagent (L3000015, Thermo Fisher Scientific) according to the manufacturer's instructions.

2.8. CRISPR/CAS9

CRISPR/CAS9-mediated TIPE3 depletion was applied according to Zhang Feng Lab's protocol (http://www.addgene.org/crispr/zhang/). The sgRNA targeting exon 3 of TIPE3 was designed using CRISPRdirect (http://crispr.dbcls.jp/) and synthesized as follows: 5′-CACCGCTCATC AAAGATCTCGCTGC-3′ and 3'-CGAGTAGTTTCTAGAGCGACGCAAA-5'. The sgRNA was annealed and ligated into a BsmBI (Thermo Fisher Scientific)-digested lentiCRISPRv2 vector (#52961, Addgene, USA). The constructed vectors were validated by sequencing. LentiCRISPRv2-TIPE3 or lentiCRISPRv2 was co-transfected with the packaging vectors pSPAX2 (#12260, Addgene) and pMD2.G (#12259, Addgene) into 293T cells using Lipofectamine 2000 transfection reagent (Thermo Fisher Scientific) to generate lentiviruses. The supernatants containing the lentiviruses were collected and used to infect U251 cells. After infection, the cells were selected with 8 mg/mL puromycin for at least 48 h. Knockout efficacy was validated by western blot.

2.9. Flow cytometric analysis

Apoptosis was measured using an Annexin V-PE/7-AAD kit (Becton Dickinson, New Jersey, USA). Cells were harvested, washed twice with PBS, stained with Annexin V-PE/7-AAD for 10 min in the dark and analyzed using a FACSCalibur flow cytometer (Becton Dickinson). Cells that are considered viable are PE Annexin V and 7-AAD negative; cells that are in early apoptosis are PE Annexin V positive and 7-AAD negative; and cells that are in late apoptosis or already dead are both PE Annexin V and 7-AAD positive. The sum of upper right quadrant and low right quadrant were used for calculating total apoptosis rates and statistical analysis.

2.10. Mitochondrial membrane potential (ΔΨm) assay

The collapse of the Δψm is a hallmark event of early stage apoptosis. Changes in Δψm were measured by JC-1 staining (Yeasen, Shanghai, China) according to the manufacturer's instructions. Images were captured with an Olympus BX51 microscope (Olympus, Japan). The ratio of JC-1 aggregates (red fluorescence) to monomers (green fluorescence) was measured. A decrease in the ratio of red/green fluorescence intensity indicated the loss of ΔΨm.

2.11. Western blotting

Cells were lysed in RIPA buffer (Beyotime, Shanghai, China) containing PMSF (Beyotime) and protease inhibitor cocktail (Roche) for 20 min at 4 °C. Equal amounts of protein were separated on SDS-PAGE gels and transferred onto PVDF membranes (Millipore, Germeny). Membranes were blocked and then incubated with the indicated primary antibody overnight. Next, the membranes were incubated with Alex Fluor 680/790-labelled secondary antibodies (LI-COR Bioscience, USA) for 2 h. The bands were visualized with a LI-COR Odyssey Infrared Imaging System (LI-COR Biosciences). Densitometry analyses were performed with Quantity One (BioRad, USA), and the results were normalized to GAPDH or β-actin.

2.12. Immunoprecipitation

Cells co-transfected with HA-TIPE3(or myc-TIPE3) and His-p38 (or His-MT-p38) vectors were lysed in IP buffer (2 mM Tris-Cl, pH 8.0, 0.5 mM EDTA, 150 mM NaCl, 1% NP-40, 50 mM NaF, 2 mM Na_3VO_4, 4 mM Na pyrophosphate, and 25 μl protein inhibitor/ml). The lysates were incubated with 5 μg of primary antibodies or IgG (Beyotime) for 4 h at 4 °C. Then, 30 μl of Protein A/G PLUS-Agarose (sc-2003, Santa Cruz Biotechnology) was added, and the samples were incubated overnight at 4 °C. The precipitates were washed 5 times with IP buffer. Next, the beads were resuspended in 40 μl of 1.5 × loading buffer, boiled for 5 min, and centrifuged at 2500 × rpm for 1 min. The supernatants were collected and subjected to SDS-PAGE followed by western blotting.

2.13. Nuclear and cytoplasmic fractionation

Nuclear and cytoplasmic proteins were extracted using NE-PER Nuclear-Cytoplasmic Extraction Reagents (Thermo Fisher Scientific) according to the manufacturer's instructions. α/β-Tubulin and histone H3 were respectively used for cytoplasmic and nuclear loading controls.

2.14. Immunofluorescence

The tissues were fixed in 10% formalin and embedded in paraffin. Briefly, the sections were deparaffinized, hydrated and subjected to antigen retrieval in 10 mM sodium citrate (pH, 6.0). Cells were fixed in 4% paraformaldehyde for 15 min. Tissues or cells were permeabilized with 0.1% Triton X-100 for 10 min, and then blocked with 1% bovine serum albumin for 1 h. Tissues or cells then were incubated with indicated primary antibodies overnight, followed by Alexa fluor-labelled secondary antibody (Antgene, Wuhan, China). The nuclei were stained with DAPI (ANT046, Antgene). Na/K-ATPase (Abcam, ab76020) was used as cell membrane marker. Images were captured with an Olympus FV1200 confocal microscope (Olympus) or an Olympus BX51 microscope (Olympus).

2.15. Immunohistochemistry and HE staining

The samples were fixed in 10% formalin and embedded in paraffin. Briefly, the sections were deparaffinized, hydrated and subjected to antigen retrieval in 10 mM sodium citrate (pH, 6.0). Endogenous peroxidase was blocked in 3% H_2O_2 for 10 min. The sections were incubated in primary antibodies overnight, followed by HRP-labelled secondary antibody (Servicebio, China). Signals were detected using DAB staining (Servicebio), and the samples were counterstained with haematoxylin. Images were obtained using an Olympus BX51 microscope (Olympus). IHC scores were determined as follows to measure immunoreactivity: 0 for background staining, 1 for faint staining, 2 for moderate staining, and 3 for strong staining. Two independent pathologists examined and scored the slides. Scores 0–1 were considered low expression, and scores 2–3 were considered high expression. The slides were stained with HE according to a standard protocol.

2.16. TUNEL assay

DNA fragmentation in apoptotic cells was measured using the In Situ Cell Death Detection Kit, according to the manufacturer's protocol (Roche). Images were obtained with an Olympus BX51 microscope (Olympus).

2.17. Intracranial xenograft model

U251-CTRL or U251-CRISPR-TIPE3 cells were resuspended in PBS at a concentration of 1×10^5 cells/μL for stereotactic implantation into the right striatum of 6-week-old Balb/c nude mice. The mice were anaesthetized with an intraperitoneal injection of 1% sodium pentobarbital. Then, the skull was drilled with a needle tip 3.5 mm from the cerebral midline and 2 mm frontal to the coronal suture. Ten microlitres of the cell suspension was injected at a depth of 3 mm from the brain surface. For the survival analysis, the mice were monitored periodically and sacrificed when they showed severe neurological symptoms and/or obvious weight loss (> 20% of their body weight). Whether the mice were moribund or not, 10 weeks post-injection was considered as the terminal point. The whole brains of the mice were removed, fixed in 4% paraformaldehyde, and embedded in paraffin for further analysis. All experiments with animals were approved by the Institutional Animal

Care and Use Committee at Renmin Hospital of Wuhan University.

2.18. Statistical analysis

The results are representative of the three independent experiments and presented as the mean ± SD. Statistical analyses were performed with SPSS version 19.0 and GraphPad Prism 5. Unpaired Student t tests were used to compare the means of two groups. One way analysis of variance was used for comparison among the different groups. When analysis of variance was significant, post hoc testing of differences between groups was performed using Student-Newman-Keuls test. The chi-square test was used for analysing the relation between TIPE3 expression and clinical parameters or level of p-p38. The Kruskal-Wallis test was used for analysing the differences in IHC scores in the tissues, followed by multiple comparison using Dunn's post-hoc test. Log rank test was used for survival analysis. Pearson test was used for analyzing the correlation between TIPE3 and other genes. $^*P < 0.05$ was considered statistically significant.

3. Results

3.1. TIPE3 is upregulated in human GBM and predicts poor prognosis

We first analyzed the expression profiles of TIPE3 in various human cancers from public TCGA database (http://cancergenome.nih.gov/). Among 17 types of human tumours, TIPE3 expression in low grade glioma and GBM are at a relatively high levels (Fig. 1A). We examined TIPE3 mRNA levels in 10 non-tumor tissue and 19 GBM tissue samples from patients. The results showed significantly higher TIPE3 mRNA levels in GBM than in non-tumor tissues (Fig. 1B). Western blot showed higher TIPE3 protein levels in 4 GBM tissues than in 4 non-tumor tissues (Fig. 1C). Next, we detected TIPE3 protein expression by IHC analyses. We found that TIPE3 protein levels were markedly higher in GBM than in adjacent nontumour brain from the same patient (Fig. 1D). We measured TIPE3 expression in 3 non-tumor tissues and 83 glioma tissue samples (WHO I, n = 2; WHO II, n = 15; WHO III, n = 25; WHO IV, n = 41). WHO I and II samples were graded as low-grade gliomas. WHO III and IV were graded as high-grade gliomas. The results demonstrated that TIPE3 expression is higher in high-grade glioma tissues than in non-tumor tissues and that high-grade gliomas have higher TIPE3 expression than low-grade gliomas, and the difference of TIPE3 expression between low-grade glioma and non-tumor was not statistically significant (Fig. 1E and F). TIPE3 expression was significantly associated with the pathological grades of glioma patients (P = 0.0013) (Table 1). To test whether *TIPE3* might predict outcomes of patients, we performed survival analysis of TCGA data (n = 488) using GlioVis platform [26]. And the results indicated that patients with high TIPE3 expression had poorer survival times (Fig. 1G). These results indicate that TIPE3 is upregulated in human glioblastomas and predicts poor prognosis.

3.2. TIPE3 knockdown induces GBM cell apoptosis in vitro

To explore the role of TIPE3 in GBM, we performed loss-of-function studies in U251 and U87 cell lines. Different siRNAs targeting TIPE3 (siTIPE3-1 and siTIPE3-2) were generated, and their knockdown efficacies were verified by western blot (the first band in Fig. 2E). First we performed TUNEL staining and cleaved-caspase3 staining to evaluate cell death. TIPE3 knockdown groups showed higher TUNEL-positive proportion than the control group in U251 and U87 cells (Fig. 2A and Supplementary Fig. 1A). GBM cells showed elevated cleaved-caspase3 levels after TIPE3 knockdown (Fig. 2B and Supplementary Fig. 1B). And Annexin V-PE/7-AAD staining demonstrated that TIPE3 knockdown induced apoptosis in U251 and U87 cells (Fig. 2C). Loss of ΔΨm is a hallmark event of the early stage of apoptosis. JC-1 staining showed that TIPE3 knockdown induced the loss of ΔΨm in GBM cells (Fig. 2D and Supplementary Fig. 1C). Moreover, we overexpressed exogenous TIPE3 in U87 cells with TIPE3 knockdown and found that exogenous TIPE3 reversed the effect of TIPE3 depletion on cell apoptosis (Supplementary Fig. 2).

3.3. TIPE3 inhibits p38 phosphorylation and regulates apoptosis-related genes in vitro

Since MAPK pathway plays an important role in regulating cell survival and death, we conducted a GSEA using glioma patient gene profiling data (GSE4290), and as shown (Supplementary Fig. 3A), TIPE3 may regulate gene sets associated with MAPK pathway. Further, we detected the activation levels of three main MAPK pathway: p38 pathway, ERK pathway and JNK pathway. The results showed ERK pathway and JNK pathway remained unchanged after TIPE3 depletion (Supplementary Fig. 3B). So we tend to examine the expression levels of p38, p-p38 and downstream apoptosis-related proteins. Our experiments revealed that TIPE3 knockdown increased p-p38 levels (Fig. 2E), and TIPE3 overexpression decreased p-p38 levels (Fig. 2F). And total p38 levels remained unchanged. Moreover, TIPE3 knockdown increased Bax, Bad and cleaved-caspase-3 levels and decreased Bcl-2 levels (Fig. 2E). TIPE3 overexpression decreased Bax and cleaved-caspase-3 levels and increased Bcl-2 and Bcl-XL levels (Fig. 2F). Based on the above results, we speculate that TIPE3 may inhibit cell apoptosis by inactivating p38 MAPK pathway.

3.4. TIPE3 inversely correlates with p38 phosphorylation and apoptosis in clinical glioma

Then we verified relationship of TIPE3, cell apoptosis and p38 phosphorylation in clinical samples. We found that TIPE3 levels correlate with a series of anti-apoptotic gene (BCL2, Bcl-XL, Bcl-w, Bfl-1, MCL-1, XIAP, c-IAP1 and c-IAP2) in 274 glioma patients from GlioVis platform (Fig. 3A). In human GBM tissues, we examined the expression of TIPE3 and p-p38 by IHC, as well as cell death by TUNEL staining. The result showed that TIPE3 expression inversely correlate with p-p38 levels and cell death in GBM tissues (Fig. 3B). A negative correlation between tumor TIPE3 and p-p38 staining was evident (Fig. 3C). And this correlation of TIPE3 and p-p38 in GBM was also confirmed by western blots (Fig. 3D).

3.5. TIPE3 associates with p38 and the nulear translocation of p38 is blocked by TIPE3 overexpression

To investigate the mechanism through which TIPE3 regulates the p38 MAPK pathway, we used immunofluorescence and co-immunoprecipitation assays to verify the potential association between TIPE3 and p38. At first, we examined the subcellular localization of endogenous TIPE3 in GBM cells. We found that TIPE3 was expressed in cytoplasm, cellular membrane and nucleus, but mainly in cytoplasm (Supplementary Fig. 4). Then we observed the co-localization of TIPE3 and p38 in GBM patient tissues (Fig. 4A), as well as the co-localization of exogenous TIPE3 and p38 in 293T cells (Fig. 4B), and the co-localization existed mainly in the cytoplasm. Co-immunoprecipitation confirmed the association between TIPE3 and p38 (Fig. 4C). These results suggest that TIPE3 associates with p38. In addition to full length TIPE3 (NCBI Reference Sequence: NM_207381.3), a transcript variant (NM_001311175.1) encodes a short-TIPE3 which has a shorter N-terminus (Fig. 4E). We constructed this short-TIPE3 vector and performed the co-IP assay. The results showed that this short-TIPE3 with a shorter N-terminus cannot associates with p38 (Fig. 4D).

P38 exists in both the nucleus and cytoplasm, and the cytoplasmic-nuclear translocation of p38 plays an important role in regulating p38 MAPK pathway activity [27]. Under basal conditions, p38 resides in the cytoplasm in its nonphosphorylated inactive state. Upon activation, p38 translocates into the nucleus and activates its downstream signalling

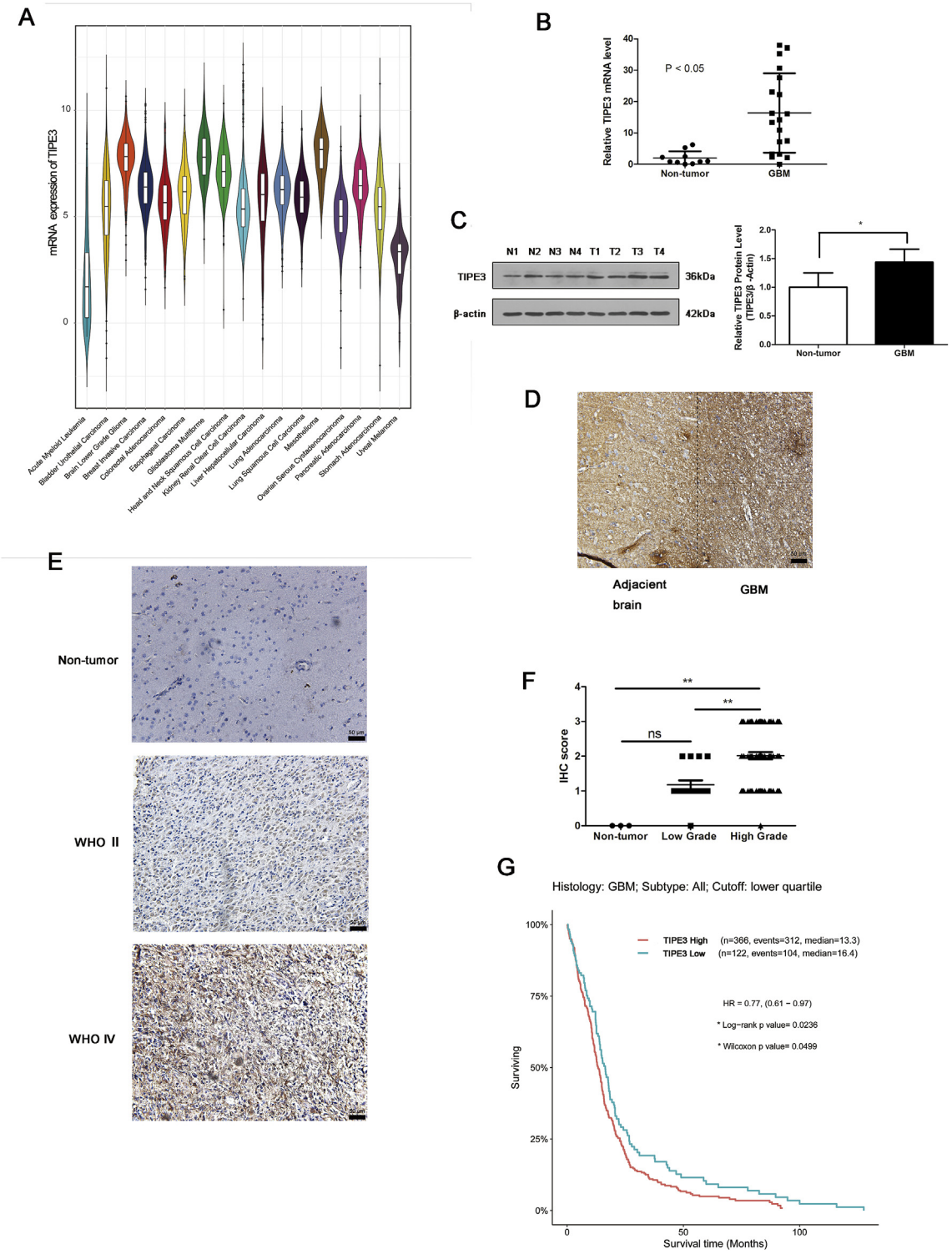

Fig. 1. TIPE3 is upregulated in human GBM and predicts poor prognosis. (**A**) Expression profiles of TIPE3 in a variety of human cancers from TCGA database. (**B**) Real-time qPCR indicated significantly higher TIPE3 mRNA levels in GBM (n = 19) tissues compared to non-tumor (n = 10) tissues. TIPE3 mRNA expression was normalized to GAPDH using the 2-ΔΔCt method. *P < 0.05. (**C**) Western blotting indicated higher TIPE3 protein levels in GBM (n = 4) tissues than in non-tumor (n = 4) tissues. N1 ~ N4 indicate non-tumor tissues, and T1 ~ T4 indicate GBM. *P < 0.05. (**D**) IHC staining of TIPE3 protein expression in GBM and the adjacent brain tissues. Scale bars, 50 μm. (**E**) Representative IHC staining images for TIPE3 in clinical tissues. Grade II and grade IV indicate the pathologic grades of the glioma samples. Scale bars, 20 μm. (**F**) IHC score of TIPE3 in clinical tissues. The IHC scores were graded as 0, 1, 2 and 3. Non-tumor tissue, n = 3; Low-grade glioma (WHO I and WHO II), n = 17; High-grade glioma (WHO III and WHO IV), n = 66. **P < 0.01. ns, not significant. (**G**) Kaplan-Meier survival analysis for TIPE3 expression in GBM patients (n = 488) from TCGA database. The data was analyzed by the GlioVis platform. P-values were obtained from Student's *t*-test (**B** and **C**), The Kruskal-Wallis test followed by multiple comparison using Dunn's post-hoc test (**F**), log-rank test (**G**). All bar plot data are the means ± SD.

Table 1
Correlation between the clinicopathological characteristics and expression of TIPE3 in glioma.

Characteristic	Number of cases	TIPE3 expression		P-value
		Low(0&1)	High(2&3)	
Gender				0.2535
Male	38	14	24	
Female	36	18	18	
Age				0.9048
≥60	26	11	15	
< 60	48	21	27	
WHO Grades				0.0013
I + II	17	13	4	
III + IV	66	22	44	

pathway [28]. We examined the effect of TIPE3 on the subcellular localization of p38 using immunofluorescence and nuclear-cytoplasmic extraction experiment. We found that TIPE3 overexpression decreased nuclear p38 levels and increased cytoplasmic p38 levels (Fig. 4F and G); TIPE3 co-localized with cytoplasmic p38 in U251 cells (Fig. 4G), which corresponds to our previous results. We also detected the subcellular localization of p-p38 in U251 cells transfected with exogenous TIPE3 or control vectors. p-p38 mainly resided in the nucleus with the absence of HA-TIPE3. Upon TIPE3 overexpression, p-p38 mainly localized in the cytoplasm, and total p-p38 levels were decreased (Fig. 4H). Notably, TIPE3 overexpression led to dramatic decreased levels of nuclear p-p38. In addition, TIPE3 co-localized somewhat with cytoplasmic p-p38 (Fig. 4H). These results indicate that TIPE3 inhibits p38 nuclear translocation. This process inactivates p38 MAPK pathway and regulates its downstream target genes.

3.6. The phosphorylation status of p38 is a regulator for TIPE3-mediated p38 nuclear-cytoplasmic translocation but does not affect the association between TIPE3 and p38

Next, we attempted to clarify the regulatory factors mediating p38 associating with TIPE3 and nuclear-cytoplasmic translocation. The phosphorylation of p38 is a hallmark event in p38 MAPK signalling pathway activation [17]. We examined whether modulating the p38 phosphorylation status could affect TIPE3-p38 association and the TIPE3-mediated nuclear-cytoplasmic translocation of p38. We constructed a phosphorylation dominant negative mutant of p38 (His-mt-p38) by changing the TGY dual phosphorylation sites of Thr180/Tyr182 to AGF. Immunoprecipitation assays revealed that this Thr180/Tyr182 mutation of phosphorylation domain does not impede the p38-TIPE3 association (Fig. 5A). We also employed BIRB796, an inhibitor of p38 phosphorylation, to confirm the role of p38 phosphorylation in p38-TIPE3 association. We found that BIRB796 had no effect on p38-TIPE3 association (Supplementary 5). These results indicated that p38 phosphorylation does not affect the association between TIPE3 and p38.

Then we tend to investigate the role of p38 phosphorylation in TIPE3-mediated p38 translocation. The results showed that the mutation of p38 phosphorylation domain reversed TIPE3-mediated p38 nuclear-cytoplasmic translocation (Fig. 5B and C).We employed two different p38 MAPK inhibitors, SB203580 and BIRB796, to assess whether p38 phosphorylation or its kinase activity can control TIPE3-mediated p38 translocation. SB203580 blocked the kinase activity of p38 but not its phosphorylation. BIRB796 blocked the phosphorylation of p38 without affecting its kinase activity [29]. The results demonstrated that BIRB796, but not SB203580, reversed the p38 nuclear translocation induced by TIPE3 knockdown (Fig. 5D and E). Thus, we speculate that it is the phosphorylation status of p38, not its kinase activity, that regulates TIPE3-mediated p38 nuclear-cytoplasmic translocation.

In summary, with the applications of p38 inhibitor and p38 phosphorylation mutant, we deduced that the phosphorylation status of p38 does not affect the association between TIPE3 and p38, but TIPE3-mediated p38 nuclear-cytoplasmic translocation is regulated by the phosphorylation status of p38, at least in some degree.

3.7. The p38 MAPK pathway is required for the regulation of glioblastoma cell apoptosis mediated by TIPE3

To further verify the hypothesis that TIPE3 inhibits glioblastoma cell apoptosis through the p38 MAPK signalling pathway, we employed p38 phosphorylation inhibitor, BIRB796, to perform the rescue experiment. BIRB796 reversed the effects of TIPE3 knockdown on cell apoptosis in U251 (Fig. 6A, D and 6G).Then, we overexpressed wild type p38 or phosphorylation negative mutant p38 to perform rescue experiments. Flow cytometry and western blotting revealed that wild type p38 (Fig. 6B, E and 6H) but not phosphorylation mutant p38 (Fig. 6C, F and 6I) reversed TIPE3-mediated cell survival in U251 cells. These results confirm that the p38 MAPK pathway is required for the regulation of glioblastoma cell apoptosis mediated by TIPE3, and modulation of p38 phosphorylation status is critical to this process.

3.8. TIPE3 depletion induces cell apoptosis in an intracranial xenograft model

We also tested whether TIPE3 depletion could induce glioblastoma cell apoptosis using an intracranial xenograft model in vivo. First, we used CRISPR/CAS9 to generate stable TIPE3 knockout GBM cells, and the knockout efficacy was validated by western blot (Fig. 7A). Second, we generated an intracranial xenograft model by implanting U251 cells intracranially. As expected, the mice implanted with the control U251 cells developed larger tumours than the mice implanted with the TIPE3 knockout cells (CRISPR-TIPE3) (Fig. 7B). TUNEL staining and IHC analyses revealed that TIPE3 depletion caused severe cell death as well as increased caspase-3 expression and decreased Bcl-2 expression (Fig. 7C). Also, p-p38 levels increased after TIPE3 depletion in vivo (Fig. 7C). Kaplan-Meier curves showed that the TIPE3 knockout group mice survived significantly longer than the control group (Fig. 7D).These results demonstrate that TIPE3 depletion enhances p38 phosphorylation and induces glioblastoma cell apoptosis in vivo.

4. Discussion

TIPE3 has been shown to be a novel regulator of human cancer [6–8], but the expression and biological role of TIPE3 in GBM is unclear. In this study, we found that TIPE3 is upregulated in GBM and that TIPE3 depletion induces GBM cell apoptosis both in vitro and in vivo. Mechanism studies reveal that TIPE3 inhibits p38 phosphorylation. TIPE3 associates with p38. The nuclear translocation of p38 is blocked by TIPE3 overxpression. The phosphorylation status of p38 is a regulator for TIPE3-mediated p38 nuclear-cytoplasmic translocation but is not required for TIPE3-p38 association. p38 MAPK pathway regulation is crucial to TIPE3-mediated cell survival in GBM.

Expression pattern of TIPE3 in brain tumour is unclear in previous studies. We examined the expression of TIPE3 in non-tumor brain tissues and gliomas and found that TIPE3 is upregulated in GBM. Notably, the non-glioma tissues were collected during surgery of severe traumatic brain injury. Whether the expression of TIPE3 could have been affected by brain tissue injury or not will be an interesting topic in our further studies.

Apoptosis evasion is a hallmark of most malignant tumours [4]. Many antitumour drugs are designed to induce apoptosis, but cell apoptosis deregulation allows GBM to avoid the apoptotic effect of these drugs, resulting in chemoresistance and treatment failure [30,31]. Previous studies have focused on the role of TIPE3 in malignant tumor transformation, cell proliferation, migration and metastasis in breast, lung, bladder and colorectal cancer [6–8]. However, little is known

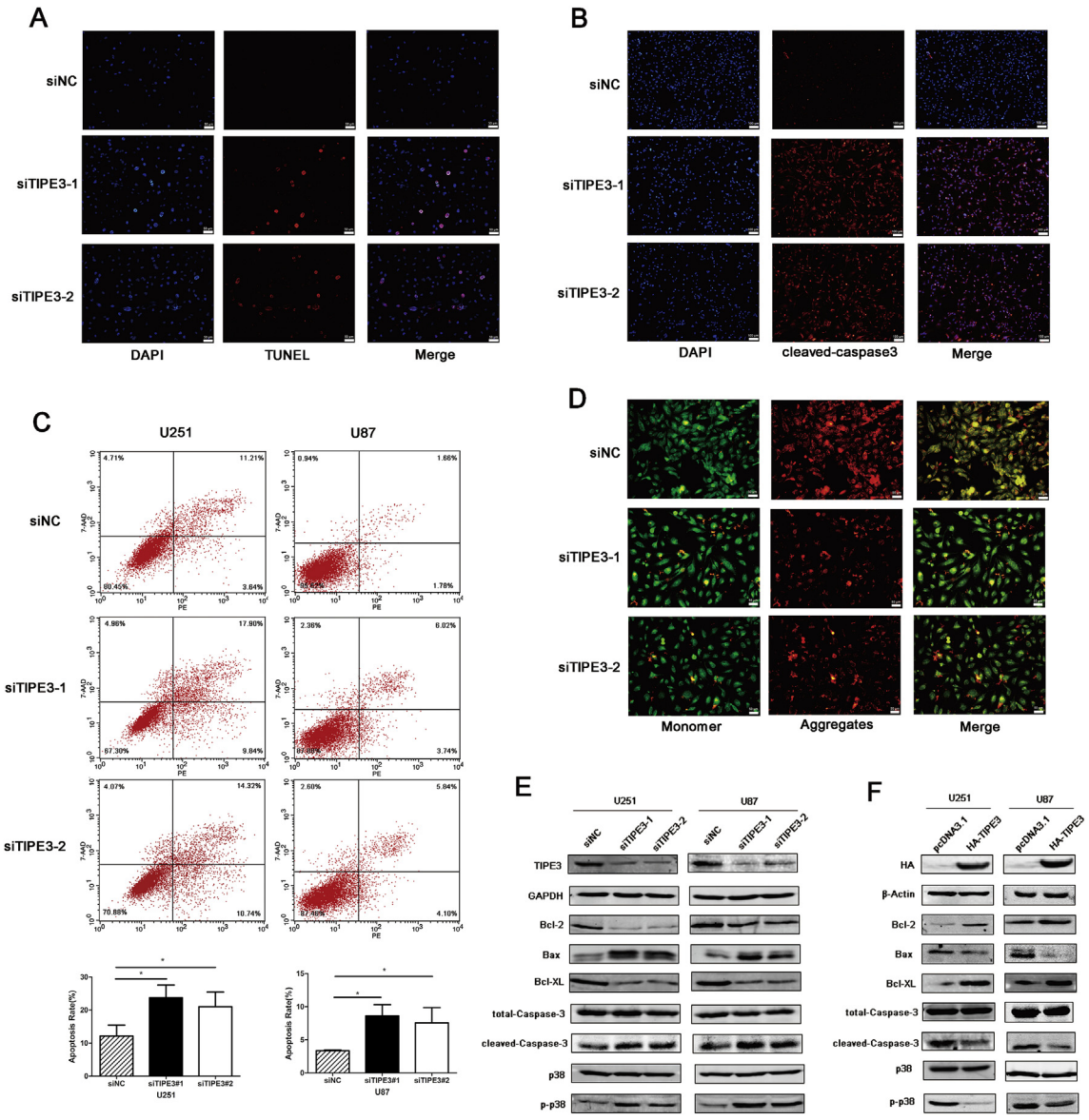

Fig. 2. TIPE3 regulates glioblastoma cell apoptosis and inhibits p38 phosphorylation in vitro. (**A**) U251 cell death were detected by TUNEL staining. Scale bars, 50 μm. Statistical analysis was showed in Fig. S6A. (**B**) Effects of TIPE3 knockdown on cleaved Caspase-3 expression in U251 cells according to immunofluorescence. Scale bars, 100 μm. (**C**) U251 and U87 cells were transfected with negative control siRNA (siNC) or siRNAs against TIPE3 (siTIPE3-1 and siTIPE3-2), followed by Annexin V-PE/7-AAD staining and flow cytometric analysis. Cell apoptosis was calculated by FACS. *P $<$ 0.05. (**D**) Effects of TIPE3 knockdown on the ΔΨm in U251 cells according to JC-1 staining. A decrease in the ratio of red (aggregates)/green (monomers) fluorescence intensity indicates the loss of ΔΨm. Scale bars, 50 μm. (**E**) Effects of TIPE3 knockdown on the levels of p-p38, p38 and its downstream apoptosis-related proteins in GBM cells. siNC: negative control siRNA. siTIPE3-1 and siTIPE3-2: two siRNAs against TIPE3. (**F**) Effects of TIPE3 overexpression on the levels of p-p38, p38 and its downstream apoptosis-related proteins in GBM cells. pcDNA3.1: the control group. HA-TIPE3: TIPE3 overexpression group. All bar plot data are the means ± SD. The data and graphs are representative of three independent experiments with similar results. (For interpretation of the references to color in this figure legend, the reader is referred to the Web version of this article.)

about the effect of TIPE3 on cell apoptosis in GBM. Our results show that TIPE3 depletion induces GBM cell apoptosis both in vitro and in vivo, indicating that TIPE3 might be a possible target in targeted molecular therapy.

Perturbations in p38 MAPK pathway are frequently associated with the deregulation of cell death and survival [32,33]. p38 is reportedly required for fluorouracil-induced cell apoptosis [34]. The effect of p38 MAPK pathway can be modulated through transcriptional and post-transcriptional mechanisms; these effects regulate the cell death and survival pathway and pro-apoptotic and anti-apoptotic proteins, such as Bcl-2 family proteins and caspase family proteins [15,35]. Our study demonstrated that TIPE3 regulates cell apoptosis.

The proteins in a signalling transduction network often form a complex to ensure that the signalling transduction is efficient, accurate and regulatable. We performed co-IP and immunofluorescence assays to confirm the association between TIPE3 and p38. However, whether TIPE3 binds to p38 directly or TIPE3 forms a complex with p38 through the existence of other scaffold proteins in a indirect way is still not clear. Further experiments to verify the direct interaction and the searching for possible scaffold protein which connects TIPE3 with p38 are needed in further study.

The subcellular localization of p38 plays an important role in activating p38 MAPK pathway [36]. Most studies report that p38 nuclear translocation is a critical cellular response to cellular stress. Upon cellular stress such as UV exposure and DNA damage, activated p38 is transported into the nucleus to induce downstream cascade

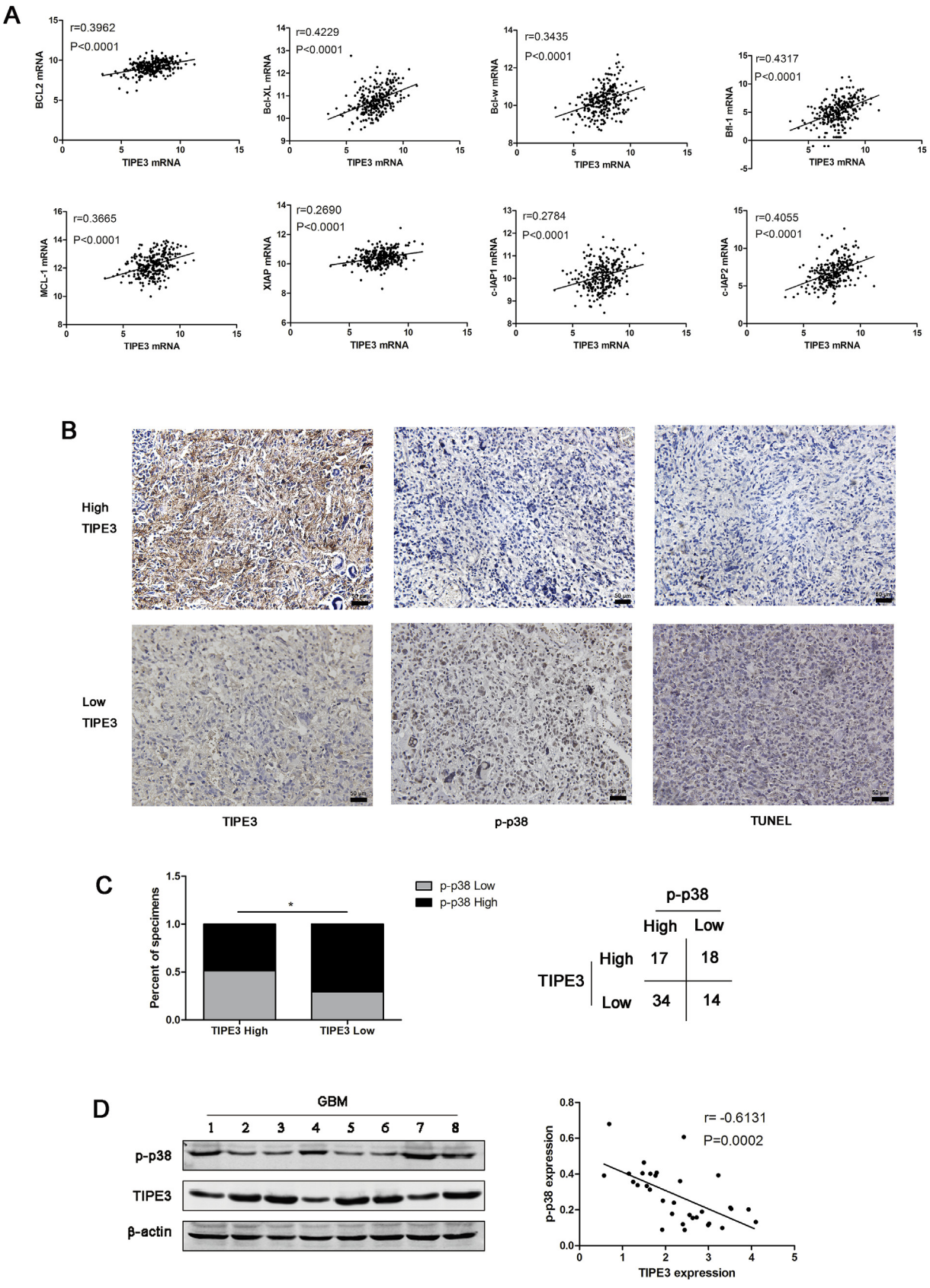

Fig. 3. TIPE3 inversely correlates with p38 phosphorylation and apoptosis in clinical glioma. (**A**) The association between TIPE3 and a series of anti-apoptotic gene (BCL2, Bcl-XL, Bcl-w, Bfl-1, MCL-1, XIAP, c-IAP1 and c-IAP2) in glioma patients (n = 274) was analyzed by the GlioVis platform. P-values were obtained from Pearson correlation. (**B**) Representatives of IHC and TUNEL staining showed TIPE3 expression inversely correlates with p-p38 and cell death in GBM tissues. Scale bars, 50 μm. (**C**) Inverse correlations of IHC data for high or low TIPE3 expression relative to level of p-p38. *P < 0.05 (**D**) Levels of TIPE3 and p-p38 were detected by western blot in 32 GBM tissues. Representive image of immunoblotting was provided. Pearson test was used for analyzing the correlation between TIPE3 and p-p38. β-actin was used as loading control.

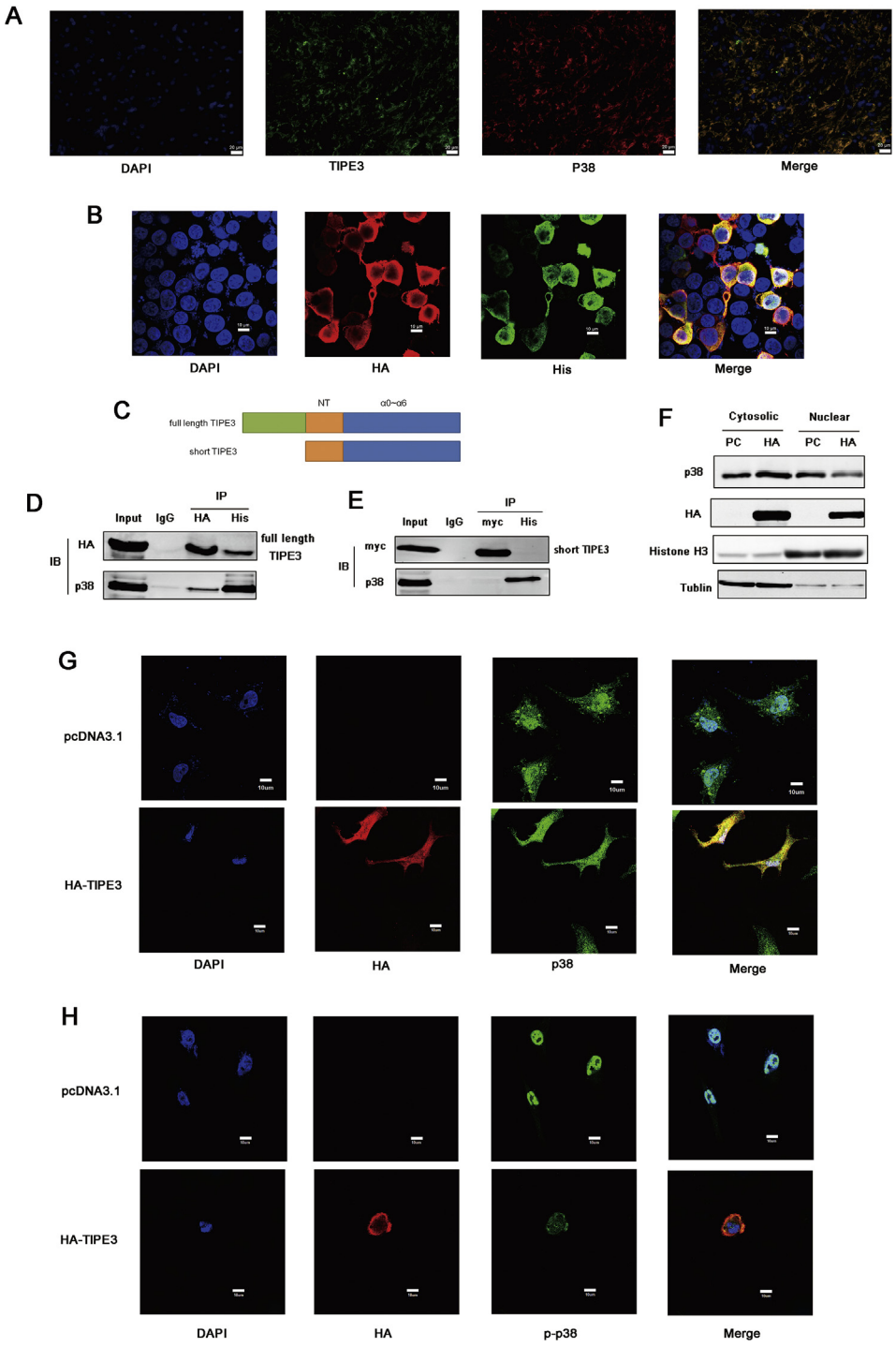

Fig. 4. TIPE3 associates with p38 and the nuclear translocation of p38 is blocked by TIPE3 overexpression. (**A**) Co-localization of TIPE3 and p38 in GBM patient tissues. Scale bars, 20 μm. (**B**) Exogenous TIPE3 and p38 co-localization was assessed by anti-HA (red) and anti-His (green) immunofluorescence staining in 293T cells co-transfected with HA-TIPE3 and His-p38 plasmids. Scale bars, 10 μm. (**C**) Schematic diagram of full length TIPE3 and short TIPE3. (**D**) Co-immunoprecipitation assays were performed to investigate the association between TIPE3 and p38. Lysates of 293T cells co-transfected with HA-TIPE3 (full length TIPE3, with HA-tag) and His-p38 plasmids were subjected to IP using anti-HA or anti-His antibodies, followed by immunoblotting with anti-HA and anti-p38 antibodies. Non-specific IgG was used as a control. Whole cell lysates were used as an input control. (**E**) N-terminal truncated TIPE3 (short TIPE3) lost its ability to associate with p38. Lysates of 293T cells co-transfected with myc-TIPE3 (short TIPE3, with myc-tag) and His-p38 plasmids were subjected to IP using anti-myc or anti-His antibodies, followed by immunoblotting with anti-myc and anti-p38 antibodies. (**F**) The nuclear and cytoplasmic fractions of U251 cells transfected with pcDNA3.1 or HA-TIPE3 were immunoblotted with anti-p38, anti-HA, anti-tubulin and anti-histone H3 antibodies. Tubulin and histone H3 were respectively used as cytoplasm and nucleus markers. (**G and H**) The effects of TIPE3 overexpression on the intracellular localization of p38 (**G**) or p-p38 (**H**) were assessed by immunofluorescence. U251 cells were transfected with pcDNA3.1 or HA-TIPE3, followed by staining with anti-HA (red) and anti-p38 (**G**) (green) or anti-p-p38 (**H**) (green). Scale bars, 10 μm. The graphs are representative of three independent experiments with similar results.

transduction [37,38]. Our study showed that TIPE3 can prevent the nuclear translocation of p38 or, in other words, promote p38 nuclear export. Given that TIPE3 can associates with p38, the possibility that TIPE3 blocks p38 nuclear translocation by interacting with p38 exists and the direct contribution of TIPE3/p38 association to the blockage of p38 nuclear translocation need to be explored in our further studies. - This possible regulation may account for the inhibitory effects of TIPE3 on the p38 MAPK pathway and cell apoptosis in part.

In addition, previous studies [6,10] have reported that TIPE3 is expressed mainly in cytoplasm and cell membrane but rarely in nucleus, and the subcellular locations of TIPE3 is related to its biological function in these studies. We observed that endogenous TIPE3 existed in cytoplasm, nucleus and cell membrane in human GBM cells (Supplementary Fig. 4), and exogenous TIPE3 existed in cytoplasm, nucleus and cell membrane (Fig. 4B, G and 4H). and both endogenous and exogenous TIPE3 existed mainly in cytoplasm. It is deduced that the subcellular locations of TIPE3 in GBM cells may lay the foundation for TIPE3 associating with p38 and mediating translocation of p38. Notably, TIPE3 has two transcript variants (NM_207381.3 and NM_001311175.1). Whether TIPE3 encoded by two transcript variants share the same or different subcellular locations is not clear. It is a interesting topic for further study.

There are three major findings in our studies. Firstly, TIPE3 inhibits p38 phosphorylation; Secondly, TIPE3 associates with p38. Thirdly, TIPE3 blocks p38 nuclear translocation. So the problem comes: what is the relationship between p38 phosphorylation, TIPE3-p38 association

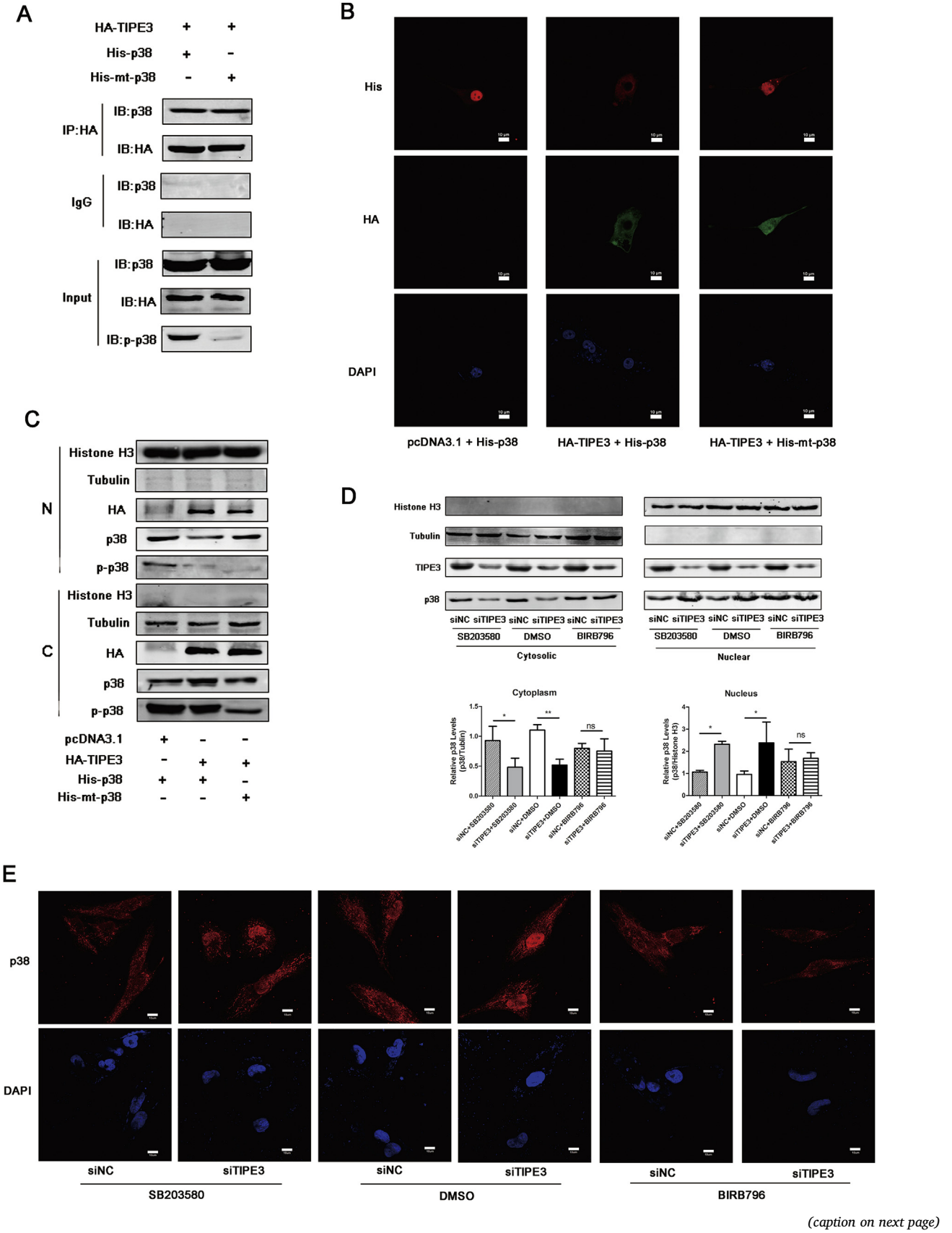

(caption on next page)

Fig. 5. The phosphorylation status of p38 affects TIPE3-mediated p38 nuclear-cytoplasmic translocation but is not required for TIPE3-p38 interaction. (**A**) Immunoprecipitation was used to assess the effect of Thr180/Tyr182 mutations on the association between TIPE3 and p38. A phosphorylation dominant negative mutant of p38 (His-mt-p38) was constructed by changing the TGY dual phosphorylation sites into AGF. Lysates of U87 cells co-transfected with the indicated plasmid groups (HA-TIPE3 + His-p38, HA-TIPE3 + His-mt-p38) were subjected to IP using an anti-HA antibody, followed by immunoblotting with anti-HA and anti-p38 antibodies. Non-specific IgG was used as a control. Whole cell lysates were used as an input control. (**B**) Immunofluorescence was used to determine the effect of Thr180/Tyr182 mutations on p38 nuclear-cytoplasmic translocation mediated by TIPE3. U87 cells were co-transfected with the indicated plasmid groups (pcDNA3.1 + His-p38, HA-TIPE3 + His-p38, HA-TIPE3 + His-mt-p38) and stained with anti-HA (green) and anti-His (red) antibodies. Scale bars, 10 μm. (**C**) A Nuclear-Cytoplasmic Extraction Kit was used to determine the effect of Thr180/Tyr182 mutations on p38 nuclear-cytoplasmic translocation mediated by TIPE3. 293T cells were co-transfected with the indicated plasmid groups (pcDNA3.1 + His-p38, HA-TIPE3 + His-p38, HA-TIPE3 + His-mt-p38). The nuclear and cytoplasmic fractions were extracted from these cells and subjected to western blot analysis. Tubulin and Histone H3 were respectively used as cytoplasm and nucleus markers. N: nuclear. C: cytosolic. (**D and E**) Effects of different p38 MAPK inhibitors on TIPE3-mediated p38 transportation were determined by Nuclear and Cytoplasmic extraction assay (**D**) and immunofluorescence (**E**). U251 cells transfected with siNC or siTIPE3 were treated with SB203580 (20 μM) or BIRB796 (1 μM) or DMSO for 24 h. Tubulin and Histone H3 were respectively used as the cytoplasm and nucleus markers. siNC: negative control siRNA. siTIPE3: siRNA target for TIPE3. The graphs are representative of three independent experiments with similar results. $P < 0.05$ was considered statistically significant.

and TIPE3-mediated p38 translocation? From the literature, the mechanism of p38 transportation is complicated and undefined. p38 phosphorylation was reportedly required for its nuclear translocation following DNA damage [37]. The nuclear export of p38 is reported to require its dephosphorylation [39]. In addition to the phosphorylation, microtubule- and dynein-dependent mechanisms were also involved in p38 nuclear translocation [39]. Because it lacks a nuclear localization sequence (NLS) and a nuclear export sequence (NES), p38 may be transported between the nucleus and cytoplasm through interacting with other proteins that have an NLS or NES. For instance, phosphorylated MAPK-activated protein kinase 2 (MK2) binds to p38; this interaction masks the NLS of MK2 and exposes the NES to cause the nuclear export of the p38-MK2 complex [40]. TAK-1-binding protein (TAB-1) binds physically to p38 and induces p38 autophosphorylation [41,42]. This action consequently prevents p38 nuclear localization [43]. TAB-1 also impedes p38 binding to MKK3 and induces p38 retention in the cytosol [43]. p38 seems to accomplish nucleus-cytoplasm transportation by forming a complex with a scaffold protein, and phosphorylation regulation may be involved in this process. It is possible that TIPE3 associates with this protein complex and mediates p38 transportation directly or indirectly. Since we have proven that TIPE3 associates with p38 and the nuclear translocation of p38 is blocked by TIPE3 overexpression, we next investigated the role of phosphorylation regulation in this process: whether the phosphorylation status of p38 affects TIPE3-p38 association, or TIPE3-mediated p38 translocation, or both?

Firstly, we found that the Thr180/Tyr182 mutation of the p38 phosphorylation domain does not impede the TIPE3-p38 association (Fig. 5A and Supplementary Fig. 5). Considering that TIPE3 can inhibits p38 phosphorylation, even though p38 phosphorylation does not affect their association, we cannot exclude the possibility that the inhibition of p38 phosphorylation might be a result of possible interaction. In further studies we plan to investigate whether TIPE3 inhibits p38 phosphorylation directly or indirectly and figure out whether TIPE3-p38 association affects p38 phosphorylation. In other words, whether the inhibition of p38 phosphorylation by TIPE3 happens before or after TIPE3-p38 association need to be explored in our further study.

Secondly, as for the relationship between p38 phosphorylation and TIPE3-mediated p38 translocation, we confirmed that the phosphorylation status of p38 affects TIPE3-mediated p38 translocation. P38 nuclear translocation induced by TIPE3 knockdown is inhibited when p38 phosphorylation is blocked (Fig. 5D and E). It is reported that p38 phosphorylation is required for its nuclear translocation following DNA damage [37], and this kind of regulation might be context-dependent and cell type specific. However, there is no agreed conclusion about how p38 phosphorylation regulates its translocation. P38 lacks NLS or NES and its translocation might be achieved through chaperons. The phosphorylation may induce a conformational change of p38, which affects its interaction with a NLS(NES)-containing chaperon, or through another protein which interacts with this NLS(NES)-containing chaperon [39]. Since our study demonstrated that p38 phosphorylation does not affect TIPE3-p38 association, we deduced that there might be another chaperon protein or some other regulatory mechanism existing. So our further study includes: verifying whether TIPE3 directly interacts with p38 or indirectly associates with p38 through another protein, searching for the existence of a possible NLS/NES in TIPE3 or the existence of third chaperon protein with a NLS/NES in the transporter complex and clarifying whether TIPE3 transports p38 directly into the cytosol or affecting p38 binding to other transfer proteins indirectly. Because we have found TIPE3 can inhibit p38 phosphorylation, it is possible that this phosphorylation inhibition may contribute to p38 cytoplasmic translocation in part. Two possible mechanisms may be responsible for the blockage of p38 nuclear translocation: on the one hand, TIPE3 associates with p38 and retains it in the cytosol, of course this hypothesis need to be verified in our further studies; on the other hand, p38 phosphorylation inhibition by TIPE3 may also contribute to the blockage of p38 nuclear translocation.

Based on the above, the inhibitory effects of TIPE3 on p38 MAPK pathway activation and its cell survival role may include two parts. Firstly, TIPE3 inhibits p38 phosphorylation which leads to p38 MAPK pathway inactivation. Secondly, TIPE3 can block its nuclear translocation, which results in p38 MAPK inactivation. TIPE3 inactivates p38 signalling pathway in more than one ways, all leading to GBM cell survival. Our rescue experiments have confirmed it (Fig. 6).

Previous studies demonstrated that TIPE3 can influence PI3K-AKT and MEK-ERK signalling pathway in NIH3T3-HRasV12 cells [6], and the possibility that the effect of TIPE3 exert on the PI3K-AKT and MEK-ERK pathway indirectly affects p38 pathway needs to be considered. Our experiments have confirmed that TIPE3 exert no effect on ERK pathway in GBM, it reminds me the role of TIPE3 in cancer might be cell-type specific. And the relationship of PI3K-AKT and p38 MAPK pathway in TIPE3-mediated regulatory system need to be clarified in our further study. Although most of studies consider TIPE3 as an oncogene, Liu et al. claimed that TIPE3 might function as a tumor suppressor in nasopharyngeal carcinoma and play a dual role in cancer progression [11]. Moreover, a study reported that plasma membrane localized TIPE3 exert opposite effect on non-small-cell lung cancer cells comparing to cytoplasimc TIPE3 [7]. There are two transcripts of TIPE3 and we found only full length TIPE3 could associate with p38 while the protein encoded by another short transcript of TIPE3 lacks this ability. What are the difference between these two transcripts? Whether the abundance of distinct transcripts determines the biological function of TIPE3 in GBM and other different human cancers? These question are the focus of our further studies. Based on other researchers' findings and our results, it is possible that more than one mechanism take part in TIPE3 regulatory system and distinct subcellular of TIPE3 may affects different core regulator of different signalling pathway.

All attempts to develop a valid small molecule to suppress p38 MAPK expression for clinical use have failed [44]. Given the ubiquitous expression of p38 and its critical role in cell signalling, it is not surprising that most p38 MAPK inhibitors, which are designed to compete with ATP and inhibit p38's catalytic activity under all conditions, result

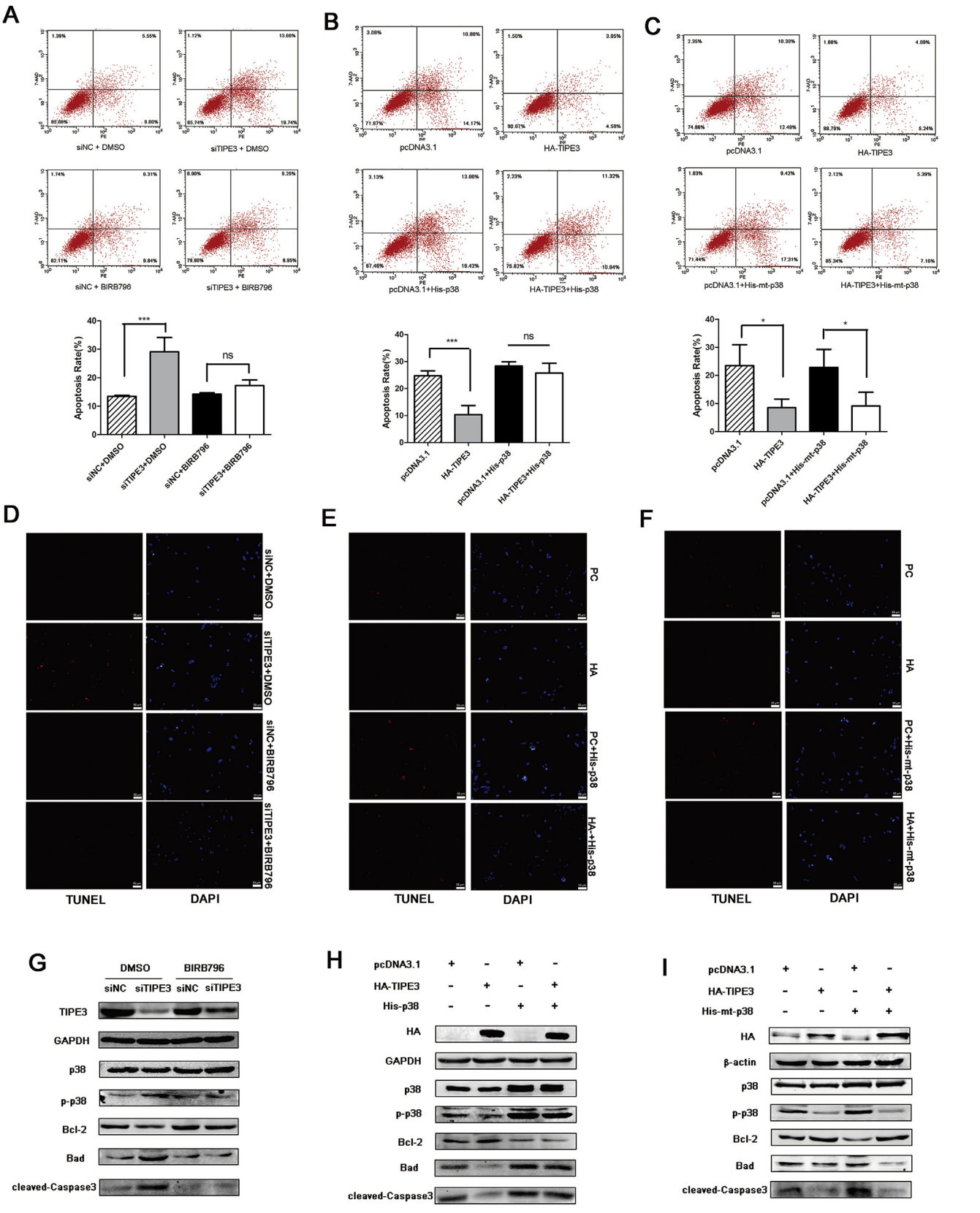

(caption on next page)

in severe side effects. Our study defines TIPE3 as a novel negative regulator of p38 MAPK pathway. Designing molecular therapy target for TIPE3 might be a possible method to suppress p38 MAPK and malignant progression of GBM. Thus, we need to thoroughly investigate the factors controlling this regulatory mechanism in future studies.

In summary, we propose a model in which TIPE3 regulates the p38 MAPK pathway and cell apoptosis (Fig. 7E). Upon external stress such as DNA damage or hypoxia, a cascade reaction leads to the

Fig. 6. The p38 MAPK pathway is required for the regulation of glioblastoma cell apoptosis by TIPE3. (**A and D**) p38 phosphorylation inhibitor BIRB796 rescued cell apoptosis induced by TIPE3 knockdown. U251 cells were pre-treated with BIRB796 at 1 μM for 24 h. Cell apoptosis was determined by FACS (**A**) and TUNEL staining (**D**). Scale bars, 50 μm. (**B and E**) TIPE3-mediated cell survival was reversed by p38 overexpression in U251 cells. Cell apoptosis was determined by FACS (**B**) and TUNEL staning (**E**). Scale bars, 50 μm. PC: pcDNA3.1. HA: HA-TIPE3. (**C and F**) TIPE3-mediated cell survival cannot be reversed by phosphorylation negative mutant of p38 (His-mt-p38) in U251 cells. Cell apoptosis was determined by FACS (**C**) and TUNEL staining (**F**). Scale bars, 50 μm. PC: pcDNA3.1. HA: HA-TIPE3. (**G**) p38 phosphorylation inhibitor BIRB796 reversed the effects of TIPE3 knockdown on apoptosis-related proteins in U251 cells. Western blot analyses were used to determine the levels of p38, p-p38, Bad, Bcl-2, cleaved-caspase-3, TIPE3 and GAPDH. (**H**) p38 upregulation reversed the effects of TIPE3 overexpression on apoptosis-related proteins in U251 cells. Western blot analyses were used to determine the levels of p38, p-p38, Bad, Bcl-2, cleaved-caspase-3, HA-TIPE3 and GAPDH. (**I**) Phosphorylation negative mutant of p38 cannot reversed the effects of TIPE3 overexpression on apoptosis-related proteins in U251 cells. Western blot analyses were used to determine the levels of p38, p-p38, Bad, Bcl-2, cleaved-caspase-3, HA-TIPE3 and β-actin. All bar plot data are the means ± SD. The data and graphs are representative of three independent experiments with similar results. *P < 0.05 was considered as significant. ns, not significant. Statistical analysis of TUNEL staining was showed in Figs. S6C–S6E.

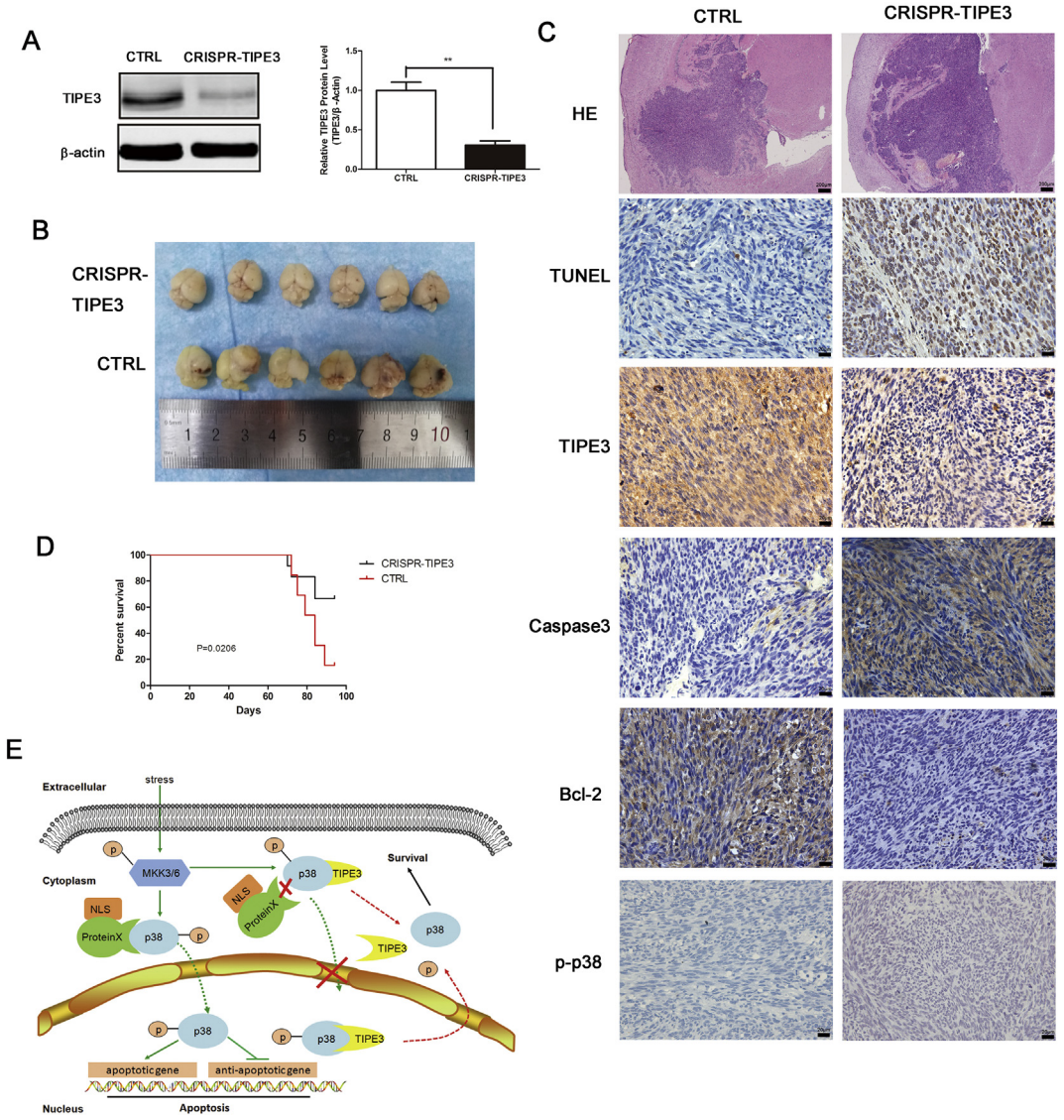

Fig. 7. TIPE3 depletion induces cell apoptosis by activating p38 MAPK pathway in an intracranial xenograft model. (**A**) The CRISPR/CAS9 system was used to generate stable TIPE3 knockout U251 cells (CRISPR-TIPE3). Knockout efficacy was assessed by western blot analysis. **P < 0.01 (**B**) Images of pLenti-CRISPR-V2 (CTRL) and pLenti-CRISPR-V2-TIPE3 (CRISPR-TIPE3) cells from mouse brains (n = 5/group). (**C**) H&E, TUNEL, and IHC analyses of TIPE3, p-p38, caspase-3, Bcl-2 and p-p38 in orthotopic tumor sections. (**D**) Mouse survival is shown by Kaplan-Meier curves. CTRL groups, n = 13. CRISPR-TIPE3 groups, n = 12. *P < 0.05. P-values were calculated using the log-rank test. (**E**) Mechanistic model for the TIPE3 regulation of cell apoptosis in GBM. All bar plot data are the means ± SD. The data and graphs are representative of three independent experiments with similar results.

phosphorylation and activation of p38. Then, phosphorylated p38 forms a complex with a transfer protein and translocates into the nucleus to activate downstream signals, resulting in cell apoptosis. As a negative regulator of p38 MAPK pathway, TIPE3 inhibits p38 phosphorylation, associates with p38 and blocks its nuclear translocation, followed by p38 MAPK pathway inactivation and cell survival. In GBM, TIPE3 is dramatically upregulated, leading to uncontrollable GBM cell survival and malignant progression. Hence, TIPE3 might be a potential therapeutic target for treating GBM.

Conflicts of interest

The authors declare that they have no conflict of interest.

Acknowledgements

This work was supported by the National Natural Science Foundation of China (No. 81572489, 81372683, and 81502175).

Appendix A. Supplementary data

Supplementary data to this article can be found online at https://doi.org/10.1016/j.canlet.2018.12.019.

References

[1] Q.T. Ostrom, L. Bauchet, F.G. Davis, I. Deltour, J.L. Fisher, C.E. Langer, M. Pekmezci, J.A. Schwartzbaum, M.C. Turner, K.M. Walsh, M.R. Wrensch, J.S. Barnholtz-Sloan, The epidemiology of glioma in adults: a "state of the science" review, Neuro Oncol. 16 (2014) 896–913.
[2] Q.T. Ostrom, H. Gittleman, L. Stetson, S.M. Virk, J.S. Barnholtz-Sloan, Epidemiology of gliomas, Cancer Treat Res. 163 (2015) 1–14.
[3] H. Mao, D.G. Lebrun, J. Yang, V.F. Zhu, M. Li, Deregulated signaling pathways in glioblastoma multiforme: molecular mechanisms and therapeutic targets, Canc. Invest. 30 (2012) 48–56.
[4] D. Hanahan, R.A. Weinberg, Hallmarks of cancer: the next generation, Cell 144 (2011) 646–674.
[5] H. Sun, S. Gong, R.J. Carmody, A. Hilliard, L. Li, J. Sun, L. Kong, L. Xu, B. Hilliard, S. Hu, H. Shen, X. Yang, Y.H. Chen, TIPE2, a negative regulator of innate and adaptive immunity that maintains immune homeostasis, Cell 133 (2008) 415–426.
[6] S.A. Fayngerts, J. Wu, C.L. Oxley, X. Liu, A. Vourekas, T. Cathopoulis, Z. Wang, J. Cui, S. Liu, H. Sun, M.A. Lemmon, L. Zhang, Y. Shi, Y.H. Chen, TIPE3 is the transfer protein of lipid second messengers that promote cancer, Cancer Cell 26 (2014) 465–478.
[7] G. Wang, C. Guo, H. Zhao, Z. Pan, F. Zhu, L. Zhang, Q. Wang, TIPE3 differentially modulates proliferation and migration of human non-small-cell lung cancer cells via distinct subcellular location, BMC Canc. 18 (2018) 260.
[8] K. Lian, C. Ma, C. Hao, Y. Li, N. Zhang, Y.H. Chen, S. Liu, TIPE3 protein promotes breast cancer metastasis through activating AKT and NF-kappaB signaling pathways, Oncotarget 8 (2017) 48889–48904.
[9] J. Cui, C. Hao, W. Zhang, J. Shao, N. Zhang, G. Zhang, S. Liu, Identical expression profiling of human and murine TIPE3 protein reveals links to its functions, J. Histochem. Cytochem. 63 (2015) 206–216.
[10] G. Wang, C. Guo, H. Zhao, Z. Pan, F. Zhu, L. Zhang, Q. Wang, TIPE3 differentially modulates proliferation and migration of human non-small-cell lung cancer cells via distinct subcellular location, BMC Canc. 18 (2018) 260.
[11] X.Y. Ren, X. Wen, Y.Q. Li, J. Zhang, Q.M. He, X.J. Yang, X.R. Tang, Y.Q. Wang, P.P. Zhang, X.Z. Chen, B. Cheng, J. Ma, N. Liu, TIPE3 hypermethylation correlates with worse prognosis and promotes tumor progression in nasopharyngeal carcinoma, J. Exp. Clin. Canc. Res. 37 (2018) 227.
[12] M.H. Rasmussen, I. Lyskjaer, R.R. Jersie-Christensen, L.S. Tarpgaard, B. Primdal-Bengtson, M.M. Nielsen, J.S. Pedersen, T.P. Hansen, F. Hansen, J.V. Olsen, P. Pfeiffer, T.F. Orntoft, C.L. Andersen, miR-625-3p regulates oxaliplatin resistance by targeting MAP2K6-p38 signalling in human colorectal adenocarcinoma cells, Nat. Commun. 7 (2016) 12436.
[13] A. Zanotto-Filho, E. Braganhol, K. Klafke, F. Figueiro, S.R. Terra, F.J. Paludo, M. Morrone, I.J. Bristot, A.M. Battastini, C.M. Forcelini, A.J. Bishop, D.P. Gelain, J.C. Moreira, Autophagy inhibition improves the efficacy of curcumin/temozolomide combination therapy in glioblastomas, Cancer Lett. 358 (2015) 220–231.
[14] H. Yang, Z.T. Gu, L. Li, M. Maegele, B.Y. Zhou, F. Li, M. Zhao, K.S. Zhao, SIRT1 plays a neuroprotective role in traumatic brain injury in rats via inhibiting the p38 MAPK pathway, Acta Pharmacol. Sin. 38 (2017) 168–181.
[15] E.F. Wagner, A.R. Nebreda, Signal integration by JNK and p38 MAPK pathways in cancer development, Nat REV CANCER 9 (2009) 537–549.
[16] L.R. Coulthard, D.E. White, D.L. Jones, M.F. McDermott, S.A. Burchill, p38(MAPK): stress responses from molecular mechanisms to therapeutics, Trends Mol. Med. 15 (2009) 369–379.
[17] X. Zou, M. Blank, Targeting p38 MAP kinase signaling in cancer through post-translational modifications, Cancer Lett. 384 (2017) 19–26.
[18] J.M. Olson, A.R. Hallahan, p38 MAP kinase: a convergence point in cancer therapy, Trends Mol. Med. 10 (2004) 125–129.
[19] H. Pang, L. Cai, Y. Yang, X. Chen, G. Sui, C. Zhao, Knockdown of osteopontin chemosensitizes MDA-MB-231 cells to cyclophosphamide by enhancing apoptosis through activating p38 MAPK pathway, Cancer Biother. Radiopharm. 26 (2011) 165–173.
[20] C.C. Chiu, J.Y. Chen, K.L. Lin, C.J. Huang, J.C. Lee, B.H. Chen, W.Y. Chen, Y.H. Lo, Y.L. Chen, C.H. Tseng, Y.L. Chen, S.R. Lin, p38 MAPK and NF-kappaB pathways are involved in naphtho[1,2-b] furan-4,5-dione induced anti-proliferation and apoptosis of human hepatoma cells, Cancer Lett. 295 (2010) 92–99.
[21] W.F. Holmes, D.R. Soprano, K.J. Soprano, Early events in the induction of apoptosis in ovarian carcinoma cells by CD437: activation of the p38 MAP kinase signal pathway, Oncogene 22 (2003) 6377–6386.
[22] M.A. de la Cruz-Morcillo, M.L. Valero, J.L. Callejas-Valera, L. Arias-Gonzalez, P. Melgar-Rojas, E.M. Galan-Moya, E. Garcia-Gil, J. Garcia-Cano, R. Sanchez-Prieto, P38MAPK is a major determinant of the balance between apoptosis and autophagy triggered by 5-fluorouracil: implication in resistance, Oncogene 31 (2012) 1073–1085.
[23] B. Zhang, T. Wu, Z. Wang, Y. Zhang, J. Wang, B. Yang, Y. Zhao, Z. Rao, J. Gao, p38MAPK activation mediates tumor necrosis factor-alpha-induced apoptosis in glioma cells, Mol. Med. Rep. 11 (2015) 3101–3107.
[24] J. Wu, H. Zhang, Y. Xu, J. Zhang, W. Zhu, Y. Zhang, L. Chen, W. Hua, Y. Mao, Juglone induces apoptosis of tumor stem-like cells through ROS-p38 pathway in glioblastoma, BMC Neurol. 17 (2017) 70.
[25] A. Glassmann, K. Reichmann, B. Scheffler, M. Glas, N. Veit, R. Probstmeier, Pharmacological targeting of the constitutively activated MEK/MAPK-dependent signaling pathway in glioma cells inhibits cell proliferation and migration, Int. J. Oncol. 39 (2011) 1567–1575.
[26] R.L. Bowman, Q. Wang, A. Carro, R.G. Verhaak, M. Squatrito, GlioVis data portal for visualization and analysis of brain tumor expression datasets, Neuro Oncol. 19 (2017) 139–141.
[27] A. Plotnikov, E. Zehorai, S. Procaccia, R. Seger, The MAPK cascades: signaling components, nuclear roles and mechanisms of nuclear translocation, Biochim. Biophys. Acta 1813 (2011) 1619–1633.
[28] T. Yokota, Y. Wang, p38 MAP kinases in the heart, Gene 575 (2016) 369–376.
[29] C. Pargellis, L. Tong, L. Churchill, P.F. Cirillo, T. Gilmore, A.G. Graham, P.M. Grob, E.R. Hickey, N. Moss, S. Pav, J. Regan, Inhibition of p38 MAP kinase by utilizing a novel allosteric binding site, Nat. Struct. Biol. 9 (2002) 268–272.
[30] C. Krakstad, M. Chekenya, Survival signalling and apoptosis resistance in glioblastomas: opportunities for targeted therapeutics, MOL CANCER 9 (2010) 135.
[31] H. Mao, D.G. Lebrun, J. Yang, V.F. Zhu, M. Li, Deregulated signaling pathways in glioblastoma multiforme: molecular mechanisms and therapeutic targets, Canc. Invest. 30 (2012) 48–56.
[32] M. Salome, A. Magee, K. Yalla, S. Chaudhury, E. Sarrou, R.J. Carmody, K. Keeshan, A Trib2-p38 axis controls myeloid leukaemia cell cycle and stress response signalling, Cell Death Dis. 9 (2018) 443.
[33] M.B. Menon, J. Gropengiesser, J. Fischer, L. Novikova, A. Deuretzbacher, J. Lafera, H. Schimmeck, N. Czymmeck, N. Ronkina, A. Kotlyarov, M. Aepfelbacher, M. Gaestel, K. Ruckdeschel, p38(MAPK)/MK2-dependent phosphorylation controls cytotoxic RIPK1 signalling in inflammation and infection, Nat. Cell Biol. 19 (2017) 1248–1259.
[34] M.A. de la Cruz-Morcillo, J. Garcia-Cano, L. Arias-Gonzalez, E. Garcia-Gil, F. Artacho-Cordon, S. Rios-Arrabal, M.L. Valero, F.J. Cimas, L. Serrano-Oviedo, M.V. Villas, J. Romero-Fernandez, M.I. Nunez, R. Sanchez-Prieto, Abrogation of the p38 MAPK alpha signaling pathway does not promote radioresistance but its activity is required for 5-Fluorouracil-associated radiosensitivity, Cancer Lett. 335 (2013) 66–74.
[35] X. Zou, M. Blank, Targeting p38 MAP kinase signaling in cancer through post-translational modifications, Cancer Lett. 384 (2017) 19–26.
[36] A. Cuadrado, A.R. Nebreda, Mechanisms and functions of p38 MAPK signalling, Biochem. J. 429 (2010) 403–417.
[37] C.D. Wood, T.M. Thornton, G. Sabio, R.A. Davis, M. Rincon, Nuclear localization of p38 MAPK in response to DNA damage, Int. J. Biol. Sci. 5 (2009) 428–437.
[38] R. Pfundt, I. van Vlijmen-Willems, M. Bergers, M. Wingens, W. Cloin, J. Schalkwijk, In situ demonstration of phosphorylated c-jun and p38 MAP kinase in epidermal keratinocytes following ultraviolet B irradiation of human skin, J. Pathol. 193 (2001) 248–255.
[39] X. Gong, X. Ming, P. Deng, Y. Jiang, Mechanisms regulating the nuclear translocation of p38 MAP kinase, J. Cell. Biochem. 110 (2010) 1420–1429.
[40] W. Meng, L.L. Swenson, M.J. Fitzgibbon, K. Hayakawa, E. Ter Haar, A.E. Behrens, J.R. Fulghum, J.A. Lippke, Structure of mitogen-activated protein kinase-activated protein (MAPKAP) kinase 2 suggests a bifunctional switch that couples kinase activation with nuclear export, J. Biol. Chem. 277 (2002) 37401–37405.
[41] D. Thapa, C. Nichols, R. Bassi, E.D. Martin, S. Verma, M.R. Conte, V. De Santis, G.F. De Nicola, M.S. Marber, TAB1-Induced autoactivation of p38alpha mitogen-activated protein kinase is crucially dependent on threonine 185, Mol. Cell Biol. 38 (2018).
[42] G.F. DeNicola, E.D. Martin, A. Chaikuad, R. Bassi, J. Clark, L. Martino, S. Verma, P. Sicard, R. Tata, R.A. Atkinson, S. Knapp, M.R. Conte, M.S. Marber, Mechanism and consequence of the autoactivation of p38alpha mitogen-activated protein kinase promoted by TAB1, Nat. Struct. Mol. Biol. 20 (2013) 1182–1190.
[43] G. Lu, Y.J. Kang, J. Han, H.R. Herschman, E. Stefani, Y. Wang, TAB-1 modulates intracellular localization of p38 MAP kinase and downstream signaling, J. Biol. Chem. 281 (2006) 6087–6095.
[44] M.L. O'Donoghue, R. Glaser, M.A. Cavender, P.E. Aylward, M.P. Bonaca, A. Budaj, R.Y. Davies, M. Dellborg, K.A. Fox, J.A. Gutierrez, C. Hamm, R.G. Kiss, F. Kovar, J.F. Kuder, K.A. Im, J.J. Lepore, J.L. Lopez-Sendon, T.O. Ophuis, A. Parkhomenko, J.B. Shannon, J. Spinar, J.F. Tanguay, M. Ruda, P.G. Steg, P. Theroux, S.D. Wiviott, I. Laws, M.S. Sabatine, D.A. Morrow, Effect of losmapimod on cardiovascular outcomes in patients hospitalized with acute myocardial infarction: a randomized clinical trial, J. Am. Med. Assoc. 315 (2016) 1591–1599.